14th International Conference on Applications of Statistics and Probability in Civil Engineering, ICASP14
Dublin, Ireland, July 9-13, 2023

Influence of Uncertain Geotechnical Data in Dynamic CPT-based Winkler Models for OWT Monopiles

Jacques Tott-Buswell
PhD Researcher, Dept. of Civil Engineering, University of Nottingham, Nottingham, United Kingdom

Joseph Hilton, Stra Berberic & Saleh Jalbi
Sea and Land Project Engineering, London, United Kingdom

Luke J. Prendergast
Assistant Professor, Dept. of Civil Engineering, University of Nottingham, Nottingham, United Kingdom

ABSTRACT: The strive to meet renewable energy targets has revealed new challenges in structural health monitoring procedures for offshore wind turbine foundations. The lack of available data on the realtime performance of monopile foundations in offshore environments has raised questions about the serviceability of monopiles after many years of operation. This requires novel approaches to ensure substructure deflections remain within serviceability limits to provide a safe and serviceable product. Dynamic models need to encapsulate damping appropriately, and one of the major contributors to a monopile's energy dissipation is due to the nonlinearity in the pile-soil interaction. This is particularly important during intense storm events where large amplitude motion will generate hysteretic behaviour in the soil. This paper details the development of a dynamic Winkler model that re-purposes monotonic CPT-based *p*-*y* functions by defining discrete hysteretic stress paths using Modified Masing's rules. The geotechnical uncertainty is investigated by generating stochastic CPT ground profiles that vary the spatial variability of the end resistance. Results demonstrate that the variability in the synthetic CPT data has a negligible effect on the performance of the nonlinear dynamic model, suggesting the influence of CPT variation in models encapsulating hysteretic damping may not be captured.

1. INTRODUCTION

The offshore wind industry has undergone significant changes in recent years, with growth driven by technological advancements and an increasing focus on renewable energy sources. In particular, monopiles have played a crucial role in the development of the industry, providing a reliable and cost-effective foundation solution and supporting 81% of Offshore Wind Turbines (OWTs) (Wind Europe, 2021). Monopiles are large tubular steel structures known for their simplicity and cost-effectiveness in design, making them an ideal solution to support new turbines and keep up with renewable energy demands. However, permissible nearshore sites are beginning to reach capacity, therefore wind harvesting infrastructure is being developed further offshore which has less certain geotechnical properties and more severe wind and wave loads.

OWTs supported by monopiles are dynamically sensitive structures and have strict design criteria for the natural frequency (Prendergast et al., 2018; Arany et al., 2017). The turbine's blade-passing (3P) and rotor (1P) frequencies impose excitation bands that must be avoided to prevent resonance

(DNV, 2016). Typically, monopiles are designed to have an overall system frequency between 1P and 3P bands (known as the soft-stiff region), and the exact design gap requirement will vary depending on the specific turbine design, operating environment, and regulatory requirements (API, 2014; DNV, 2016). Additionally, modern OWTs are increasing in tower and blade size, with only a small increase in weight. This leads to a natural frequency shift closer towards the imposed environmental loads and an increased likelihood of resonance. In this light, design practices and numerical models must account for system damping adequately to design against resonance and avoid conservative solutions. The primary contributor to energy dissipation for large amplitude cyclic loading is due to the nonlinearity in soil (Andersen, 2010; Tarp-Johansen et al., 2009). The nonlinear Dynamic Soil Structure Interaction (DSSI) can be modelled by repurposing monotonic *p*-*y* methods to inform discrete hysteretic stress paths in a Winkler model. In this paper, the backbone curves deriving the discrete hystereses are informed using *p*-*y* methods that utilise Cone Penetration Test (CPT) data. The geotechnical uncertainty associated with deep offshore environments is encapsulated using stochastic methods to formulate synthesized CPT data. The flowchart in Figure 1 demonstrates how the model will be informed. The purpose of this study is to qualitatively investigate the influence of CPT spatial variability on Winkler models with hysteretic damping.

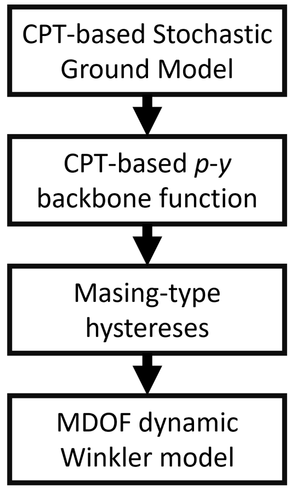

Figure 1: Simple flowchart demonstrating model workflow

2. Geotechnical Uncertainty

There are two variants to geotechnical uncertainties; (i) aleatory uncertainty, which refers to the spatial and temporal variation inherent to the soil in question, and (ii) epistemic uncertainty, which refers to uncertainty in the model itself due to a lack of knowledge or limited data (Baecher and Christian, 2003). The former is a property of the data, while the latter is a property of the model. This paper will examine the effects of spatial variation in CPT data on dynamic Winkler models by using a stochastic ground model, which is developed using the random field approach to describe the spatial variability in soil strength (Lloret-Cabot et al., 2014; Griffiths et al., 2009). The parameters required to define a random field are standard deviation, the mean, and scale of fluctuation (θ), where θ represents the average distance over which soil properties are significantly correlated (i.e. average depth between successive zones of high or low strength). This is a measurable property of soil that can be obtained either by curve fitting or an autocorrelation function to the correlation structure of a detrended CPT profile (Prendergast et al., 2018; Remmers et al., 2019; Lloret-Cabot et al., 2014). The Markov correlation function is used, and the reader is referred to Reale et al. (2021) for more information on the stochastic generation of the synthetic CPT profiles presented in Figure 2. Figure 1 describes the flowchart for the model within this paper. The synthetic CPT profiles for $\theta = 0.2$m and $\theta = 1.0$m are given in Figure 2a and 2b, respectively. Note that the means of the two profiles are the same and linearly increasing.

3. Dynamic Soil Structure Interaction modelling

In DSSI, energy can be dissipated as a result of the structure radiating energy in the form of surface waves into the surrounding soil. Known as radiation damping, this occurs during high-frequency oscillation and can be assumed negligible for frequencies below 1Hz (Andersen, 2010). However, the nonlinearity of soil leads to significant energy dissi-

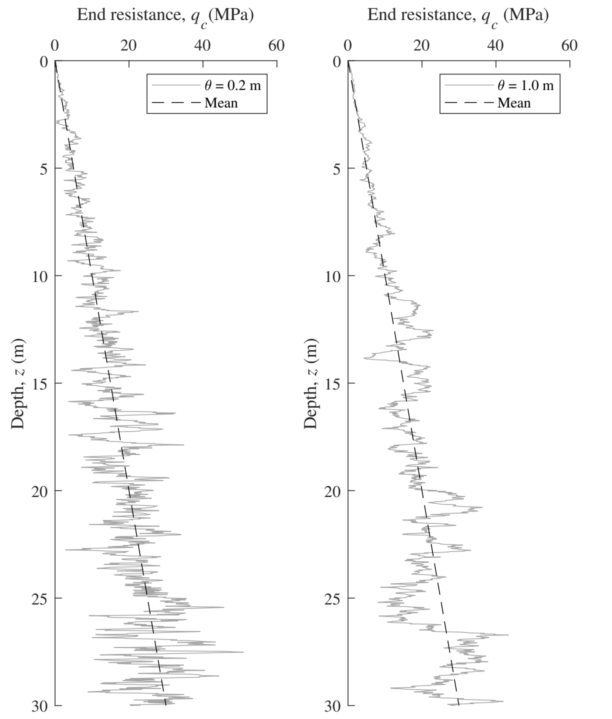

(a) (b)

Figure 2: Stochastic CPT data for (a) θ =0.2m and (b) θ =1.0m (Reale et al., 2021)

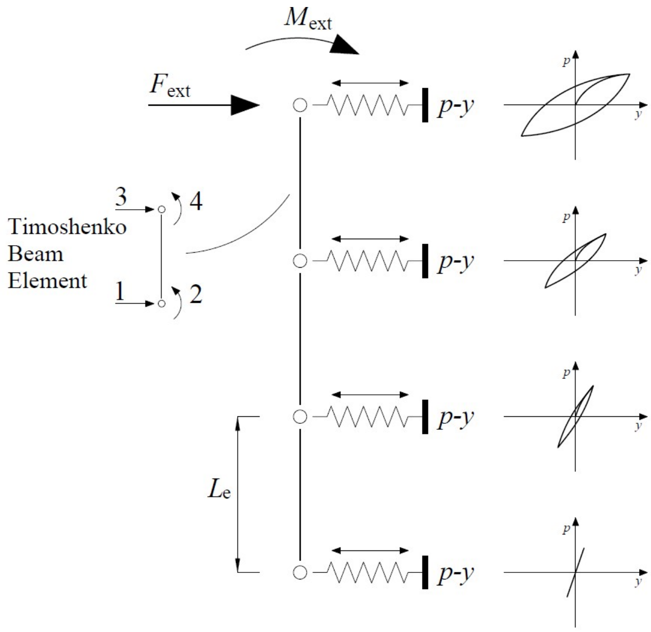

Figure 3: Winkler model with typical hysteretic behaviour

pation due to the hysteretic behaviour formed under high-amplitude cyclic loads (Badoni and Makris, 1996; Gerolymos and Gazetas, 2006). This is particularly important when modelling the performance of OWTs in extreme loading conditions. The amount of energy dissipated due to material damping is a function of the displacement amplitude rather than an intrinsic property of the soil material, therefore time-domain analysis is necessary to adequately capture the soil nonlinearity and energy dissipation of the system (Vucetic and Dobry, 1991; Ishihara, 1997). In this paper, the Constant Average Newmark Beta time marching algorithm is used due to its unconditional stability and no presence of amplitude decay (numerical damping) (Chopra, 2013), and the Modified Newton Raphson equilibrium iteration scheme is used to balance the dynamic forces at each timestep. The stress paths of discrete *p*-*y* hystereses are informed based on the well-established *p*-*y* design methodology for piles (DNV, 2016; API, 2014). An illustration of the model is shown in Figure 3.

The area within each hysteresis loop encapsulates the anticipated material damping of the discrete soil layer.

3.1. The p-y method

The *p*-*y* method is a numerical approach to analyse the behaviour of piles subject to lateral loading by discretising the soil stratum and encapsulating the soil-structure interaction with a series of nonlinear springs. Known as *p*-*y* springs, the spring response is characterised by a nonlinear function representing the soil layer's lateral pressure, p, as a function of the lateral displacement, y. The pile properties are modelled with vertical elastic Timoshenko beam elements that link the horizontal springs (Figure 3). Each synthetic q_c profile is averaged in increments of 0.5m such that $q_{c,avg}$ informs each *p*-*y* function with Equation 2 (Suryasentana and Lehane, 2016).

$$p_u = 2.4\gamma z D \left(\frac{q_{c,avg}}{\gamma z}\right)^{0.67} \left(\frac{z}{D}\right)^{0.75} \tag{1}$$

$$p = p_u \left(1 - \exp\left[-6.2\left(\frac{z}{D}\right)^{-1.2}\left(\frac{y}{D}\right)^{0.89}\right]\right) \tag{2}$$

where p_u is the ultimate resistance, γ is the unit weight, z is the spring depth, and D is the pile diameter. The unit weight of sand is taken as $20\text{kN}\,\text{m}^{-3}$. The initial shear modulus G_0 is approximated with q_c using the scaling relationship proposed by Baldi et al. (1989) as recommended in the IC-05 design method (Jardine et al., 2005), and Equation 3 is used to compute the initial stiffness of the p-y spring (Suryasentana and Lehane, 2016). The small strain Poisson ratio v_0 is taken as 0.2.

$$\left(\frac{dp}{dy}\right)_{y=0} = K_{initial} = 4G_0(1+v_0) \tag{3}$$

3.2. Hysteresis Model

The monotonic p-y functions for discrete spring elements can be repurposed to inform the backbone curve of the hysteretic stress paths if the load rate is sufficiently low (Ishihara, 1997). Therefore the discrete hystereses in Figure 3 are constructed using Modified Masing's rules (Muravskii, 2009), which scale and translate the monotonic p-y functions from Equation 2 to replicate the unload-reload branches expected in response to cyclic loading (Masing, 1926; Pyke, 1979; Vucetic, 1990; Idriss et al., 1978). The p-y hysteresis is illustrated in Figure 4 and the p-y function is modified using Equations 4 and 5.

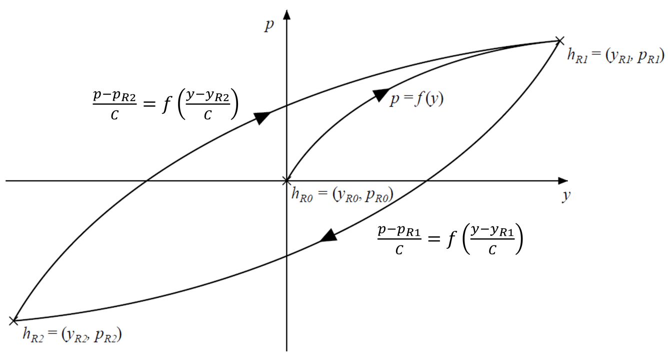

Figure 4: Modified Masing's rules modifying the backbone p-y curve

$$p = Cf\left(\frac{y-y_{R,i}}{C}\right) + p_{R,i} \tag{4}$$

$$\frac{dp}{dy} = K_T = f'\left(\frac{y-y_{R,i}}{C}\right) \tag{5}$$

The subscript R,i denotes the coordinates of the hysteretic reversal points and K_T is the tangent stiffness of the hysteresis. C is defined using Equation 6 and extends the traditional Masing rules for general asymmetrical loading (Pyke, 1979).

$$C = \left|\text{sgn}(\dot{y}) - \frac{p_u}{p_{R,i}}\right| \tag{6}$$

where $\dot{y}$ is the velocity of the pile node connected to the spring. The tangent stiffness of the p-y curve described in Equation 2 is calculated as the first derivative with respect to y and is given in equation 7.

$$\frac{dp}{dy} = \frac{5.518P_uD^{0.31}}{y^{0.11}z^{1.2}}\exp\left[-6.2\frac{D^{0.31}y^{0.89}}{z^{1.2}}\right] \tag{7}$$

3.3. Monopile Configuration

The properties of the reference monopile used in this study are given in Table 1. The loads and moments applied to the pile head are derived based on Serviceability Limit State (SLS) design compliance for an example wind turbine and are 1155kN and 93225kN m, respectively (Prendergast et al., 2018; Reale et al., 2021; Arany et al., 2017). The load and moment are arbitrarily increased by a factor of 5 to generate nonlinear behaviour in the spring elements.

Table 1: Reference monopile properties

Monopile Properties	Value
Diameter, D (m)	6
Length, L (m)	30
Wall thickness, t (m)	0.045
Density, ρ (kgm^{-3})	7850
Young's Mod., E (MPa)	210,000

The force time-history is idealised as a symmetric sinusoidal load profile to represent two-way loading with frequency 0.5Hz. Only the pile mass is considered in the mass matrix and Rayleigh damping is included with a damping ratio of 0.02. The beam element length is chosen as $L_e = 0.5$m which corresponds with the incremental average length used to determine $q_{c,avg}$ for Equation 2.

4. RESULTS AND DISCUSSION

Figure 5 shows the last loop of the hystereses for three different springs along the pile at depths 2m, 7m and 12m. The plotted depths are chosen arbitrarily to demonstrate the nonlinear soil-structure behaviour along the pile. The area within the loops appropriately reduces along the depth due to the mean q_c values linearly increasing with depth (Figure 2) as well as pile displacements varying with depth. Springs deeper than z=12m demonstrate a linear relationship and therefore exhibit no hysteretic behaviour and have no contribution to the energy dissipated in the system. The average slope of the loops also increases with depth, representative of the linearly increasing mean q_c and therefore an increase in soil stiffness. It is shown that the scale of fluctuation θ has a minor influence on the loops generated. The partial difference in the shapes is due to the backbone curves defined by Equation 2 utilising $q_{c,avg}$ over intervals of 0.5m from the synthetic CPT profiles plotted in Figure 2. Due to the random variability local to the springs, the ultimate soil pressure p_u and initial stiffness $K_{initial}$ also vary, which is captured using the Masing's Rules described in Equation 4. In general, the area encapsulated within loops for both θ values are qualitatively similar, therefore the spatial variability in CPT profiles has a negligible influence (or is not captured) on the dissipative properties of the model.

Figure 6 shows the pile head displacement for the first 10 seconds of the dynamic model simulation. The scale of fluctuation in the synthetic CPT profiles has negligible influence on the pile's displacement over time. Considering that the mean end resistance profile for each synthetic CPT strata in Figure 2 is the same, this is an intuitive result. The degree of uncertainty in CPT profiles has an insignificant effect on modelling energy dissipation through discrete Masing-type hystereses. The displacement response for θ=0.2m and θ=1.0m is the same.

5. CONCLUSION

This paper offers a qualitative study on the geotechnical uncertainties associated with dynamic Winkler models using Masing-type hysteresis damping informed through CPT-based monotonic reaction curves. The spatial variability is represented

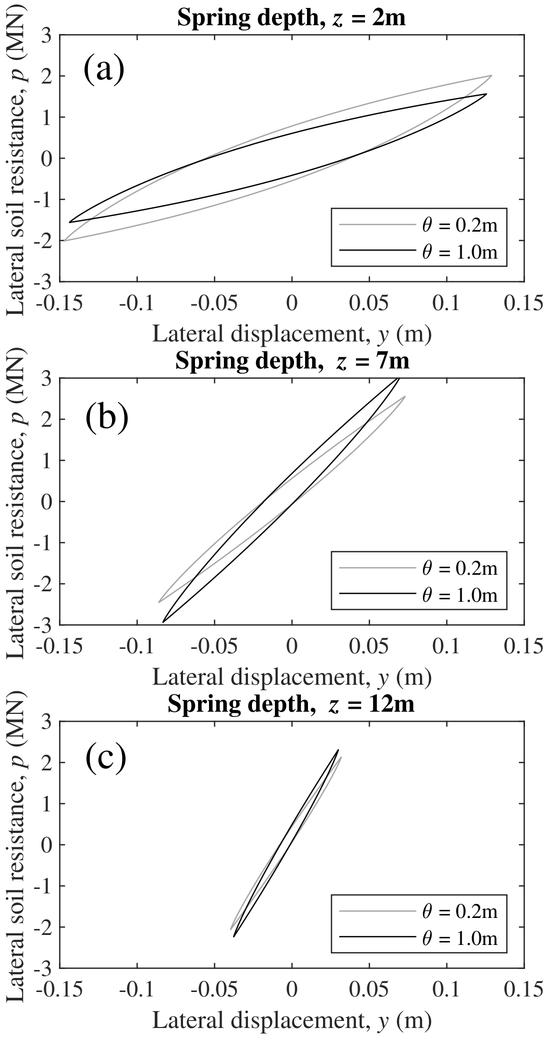

Figure 5: Hystereses for springs at depths (a) z =2m, (b) z =7m, and (c) z =12m

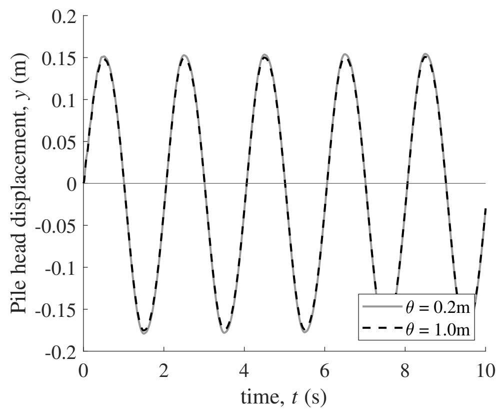

Figure 6: First 10 seconds of pile head displacement with time for both θ =0.2m and θ =1.0m

through the scale of fluctuation θ, and synthetic CPT profiles are derived using the Markov correlation function for θ =0.2m and θ =1.0m, as described in Reale et al. (2021). The mean q_c of each profile is the same. The model encapsulates a reference OWT monopile with loads derived for SLS compliance and is scaled by an arbitrary factor of 5 to generate hysteretic damping behaviour in the springs. Results show that the area of the hysteresis loops appropriately reduces along the pile depth due to the mean q_c increasing linearly with depth and varying pile displacements. The hysteresis shapes defining the spring response have minor variations with θ due to the random local variations informing the CPT-based *p-y* backbone curves. This affects the ultimate soil pressure and the initial stiffness of each spring, thereby affecting the average slope of the hysteresis. The area within the loops has minor differences; however, the net effect of the scale of fluctuation for the synthetic CPT profiles is minimal on the responses of the dynamic model, as the pile head displacement is unaffected for simple sinusoidal loading. The performance of correlation structures other than the Markov function is uncertain, and will therefore be investigated in future work.

6. ACKNOWLEDGEMENTS

The authors wish to acknowledge financial support from the Innovate UK project OfDiMoS, project number 10021835, funded under the SMART Grant October 2021 call. The first author wishes to acknowledge the EPSRC Standard Research Studentship (DTP) at the Faculty of Engineering, University of Nottingham EP/R513283/1.

7. REFERENCES

Andersen, L. (2010). "Assessment of lumped-parameter models for rigid footings." *Computers & Structures*, 88(23-24), 1333–1347.

API (2014). *RP 2GEO: Geotechnical and foundation design considerations*. Washington, DC, USA: API.

Arany, L., Bhattacharya, S., Macdonald, J., and Hogan, S. (2017). "Design of monopiles for offshore wind turbines in 10 steps." *Soil Dynamics and Earthquake Engineering*, 92, 126–152 Publisher: Elsevier.

Badoni, D. and Makris, N. (1996). "Nonlinear response of single piles under lateral inertial and seismic loads." *Soil Dynamics and Earthquake Engineering*, 15(1), 29–43.

Baecher, G. B. and Christian, J. T. (2003). *Reliability and statistics in geotechnical engineering*. J. Wiley, Chichester, West Sussex, England ; Hoboken, NJ.

Baldi, G., Bellotti, R., Ghionna, V., Jamiolkowski, M., and Lo Presti, D. (1989). "Modulus of sands from CPTs and DMTs." *Proc. 12th international conference on soil mechanics and foundation engineering, Rio de Janeiro, 1989. Vol. 1*, 165–170.

Chopra, A. (2013). *Dynamics of Structures - Theory and applications to earthquake engineering*. John Wiley & Sons, Inc., Hoboken, NJ, USA, <http://doi.wiley.com/10.1002/9781118599792> (February) Publication Title: Dynamics of Structures.

DNV (2016). "DNV-OS-J101 - Design of Offshore Wind turbine Structures. Place: Oslo: Det Norske Veritas.

Gerolymos, N. and Gazetas, G. (2006). "Development of Winkler model for static and dynamic response of caisson foundations with soil and interface nonlinearities." *Soil Dynamics and Earthquake Engineering*, 26(3), 363–376.

Griffiths, D. V., Huang, J., and Fenton, G. A. (2009). "Influence of Spatial Variability on Slope Reliability Using 2-D Random Fields." *Journal of Geotechnical and Geoenvironmental Engineering*, 135(10), 1367–1378 Publisher: American Society of Civil Engineers.

Idriss, I. M., Dobry, R., and Singh, R. D. (1978). "Nonlinear Behavior of Soft Clays during Cyclic Loading." *Journal of the Geotechnical Engineering Division*, 104(12), 1427–1447.

Ishihara, K. (1997). *Soil behaviour in earthquake geotechnics* Publication Title: Choice Reviews Online ISSN: 0009-4978.

Jardine, R. J., Chow, F., Overy, R., and Standing, J. (2005). *ICP design methods for driven piles in sands and clays*. Thomas Telford London.

Lloret-Cabot, M., Fenton, G., and Hicks, M. (2014). "On the estimation of scale of fluctuation in geostatistics." *Georisk: Assessment and Management of Risk for Engineered Systems and Geohazards*, 8(2), 129–140.

Masing, G. (1926). "Eigenspannungen und Verfestigung beim Messing [Fundamental stresses and strengthening with brass]." *International Congress of Applied Mechanics, 2d*, Zirich.

Muravskii, G. (2009). "Application of hysteresis functions in vibration problems." *Journal of Sound and Vibration*, 319(1), 476–490.

Prendergast, L., Reale, C., and Gavin, K. (2018). "Probabilistic examination of the change in eigenfrequencies of an offshore wind turbine under progressive scour incorporating soil spatial variability." *Marine Structures*, 57, 87–104.

Pyke, R. (1979). "Nonlinear Soil Models for Irregular Cyclic Loadings." *Journal of the Geotechnical Engineering Division*, GT6, 3–8 ISBN: 0815352549.

Reale, C., Tott-Buswell, J., and Prendergast, L. J. (2021). "Impact of Geotechnical Uncertainty on the Preliminary Design of Monopiles Supporting Offshore Wind Turbines." *ASCE-ASME J Risk and Uncert in Engrg Sys Part B Mech Engrg*, 7(4), 040903.

Remmers, J., Reale, C., Pisanò, F., Raymackers, S., and Gavin, K. (2019). "Geotechnical installation design of suction buckets in non-cohesive soils: A reliability-based approach." *Ocean Engineering*, 188, 106242.

Suryasentana, S. K. and Lehane, B. M. (2016). "Updated CPT-based p – y formulation for laterally loaded piles in cohesionless soil under static loading." *Géotechnique*, 66(6), 445–453.

Tarp-Johansen, N. J., Andersen, L. V., Christensen, E., Mørch, C., Kallesøe, B., and Frandsen, S. (2009). "Comparing Sources of Damping of Cross-Wind Motion." *Proceedings of European Offshore Wind 2009 : Conference & Exhibition*, 1–10.

Vucetic, M. (1990). "Normalized behavior of clay under irregular cyclic loading." *Canadian Geotechnical Journal*, 27(1), 29–46.

Vucetic, M. and Dobry, R. (1991). "Effect of Soil Plasticity on Cyclic Response." *Journal of Geotechnical Engineering*, 117(1), 89–107.

Wind Europe (2021). "Offshore wind in Europe: Key trends and statistics 2020." *Report no.*, <https://windeurope.org/data-and-analysis/product/offshore-wind-in-europe-key-trends-and-statistics-2020/>. ISSN: 14710846.